AN EXPERIMENTAL STUDY OF THE EFFECTS OF SWEPT ANGLE ON THE BOUNDARY LAYER OF THE 2D WING

A. Davari[*], M.R. Soltani[†], A.Tabrizian [‡], M.Masdari[§]

[*] Assistant Professor, Department of mechanics and Aerospace Engineering, Islamic Azad university(davariar@yahoo.com)
[†] Professor, Department of Aerospace Engineering, Sharif university of Technology(msoltani@sharif.edu)
[‡] M.S. student, Department of Aerospace Engineering, Sharif university of Technology(arshia_tabrizian@yahoo.com)
[§] Assistant Professor, Department of advanced science and technology, Tehran university(mmasdari@yahoo.com)

ABSTRACT

An experimental study was undertaken to investigate the combinational effects of angle of attack and swept angle on the boundary layer behavior of isolated swept wings. Two rectangular thin plates were attached to the wing at both the tip and the root sections to prevent the tip flow and reduce the wall boundary layer effects. And further to eliminate the wing tip vortices. Three swept wings with swept angles of 23, 33 and 40 degrees were tested. The airfoil of wings was similar to NACA 6-series airfoils. The tests were carried out at three angles of attack of -2, 0 and 2 degrees.

A 46 probe rake was used to measure the velocity profile on the wing. The measurements were performed at 3 span-wise and at 3 to 5 chord-wise positions on all wings. All tests were conducted at a constant velocity of 50 m/sec corresponding to a Reynolds number of $0.8x10^6$.

The velocity on the swept wings can be decomposed to longitudinal and cross flows. The cross flow emerges due to the non-equilibrium of pressure and centrifugal forces. To balance these two forces the outer streamlines should be curved. As the streamlines approach to the wing surface, their radius of curvature decreases. So the cross flow will appear in the vicinity of the centers of curvatures.

According to the results, as the angle of attack increases, the cross flow component decreases. The maximum cross flow in the present experiments was obtained at -2 degree angle of attack. The increase in the wing swept angle increases the cross flow strength on the wings. This is due to increase in the tangential component of the oncoming flow, as the wing swept angle increases. The results show that the cross flow strength is nearly constant at the quarter chord line of the wing. The power spectrum analysis showed a frequency mode of about 4 Hz for all conditions tested. This frequency seems to be associated with the cross flow instability. The amplitude of this frequency decreases as the angle of attack increases. It was also observed that the slope of the velocity profile near the surface was greater in the leading edge than that in the trailing edge. This slope showed that at sufficiently large values of x/C_{root}, the flow becomes turbulent.

INTRODUCTION

The swept angle and angle of attack over isolated wings is considered in this paper. In order to prevent the flow to move from lower surface to upper surface of the wing, two flat plates were placed on both ends. The boundary layer velocity profiles and instability frequencies at various cases were measured. These measurements will enable one to control or maybe postponed the transition and separation locations over the wing surface. Keeping the flow laminar over the wing has a significant effect on drag reduction and consequently fuel consumption. The three dimensional effects of the flow will remain, however, over the wing due to swept angle, even though the wing is isolated by the end plates.

The oncoming velocity over the swept wing is decomposed into tangential and normal components. The swept angles are mostly used in transonic airplanes because of velocity decomposition. And further to delay shock formation over the wing surface [7].

In addition, swept angle, reduces the C_l and $C_{l\alpha}$. due to three dimensional effects of flow, the pressure gradient and boundary layer edge velocity do not balance each other. Thus, to keep the forces balanced, the outer streamline should be curved. The equilibrium between pressure gradient and centrifugal forces is given by following equation [6].

$$\frac{\partial P}{\partial z} = \frac{\rho U^2}{R}$$

Where U is the velocity and R is the radius of curvature. The static pressure is constant across the boundary layer. Close to the surface of wing, the velocity decreases but still the pressure gradient is zero. Then, to control the equilibrium of forces the radius of curved streamlines should be decreased. Finally the velocity will be zero at the wall, no slip condition will be satisfied. As a result, when the radius of curvature is changed, cross flow will be formed toward center of curvatures. This cross flow is normal to the streamlines and is parallel to the wing surface. Strong adverse pressure gradients will not cause flow separation, because the flow can go thru the direction of lowest resistance on the wing[7].

TEST APPARATUS

All these tests were conducted in a subsonic, closed loop wind tunnel which is able to provide the velocity of 100 m/s in its test section. It has a test section with dimensions of 200x80x80 cm, and has a turbulence intensity of 0.1% which is provided thru honeycombs and several anti-turbulence screens. The velocity in test section is provided by a rotating fan. In order to control the flow temperature in test section, a refrigerating system has been applied, which is able to control the temperature between 20 and 40 °C. The models used in this experiment were made from aluminum alloy and had blockage ratio of about 8%. Upper surface of the wing has been covered with 4 rows of static pressure holes. Sections 1 to 3 are chord-wise and section 4 is span-wise. The airfoil of the models is similar to NACA 6-series airfoils which are laminar airfoils with maximum thickness located about 50% of the chord, having taper ratio and aspect ratio of 0.43 and 4 respectively.

The tests were performed with semi-span models. Using semi-span not only allow fabrication of larger models and testing at higher Reynolds number, but also causes stronger models in the test section and the acquisition process would be easier. In addition, semi-span models do not require struts [1].

To reduce the boundary layer of wind tunnel`s test section a metal thin flat plate is used at both ends of the wing [1]. In a separate project, using tuft visualization, the effect of reduction of wind tunnel boundary layer, when using the flat plate was observed and verified [2].

The major aim of this research is to investigate the three dimensional effects of flow separately, over the wing. So, a plexiglas thin flat plate is used at the tip of the wing to remove tip vortices, as shown in figure 1.

Total pressure over various ports of the wing is measured by a 46 probes rake. Each probe has internal diameter of 0.27mm and outer diameter of 0.4mm, and is connected to a pressure transducer by plastic tubes.

Due to the curvature of wing surface, it was not possible to locate the rake exactly perpendicular to the wing surface exactly. Thus, a rotating gear was designed and fabricated, as shown in figure 2. All tubes are connected to the differential type pressure transducers having pressure ranges of 1psi and 5psi. In this experiment, the 1psi sensors are used for the probes close to wing surface. All the sensors have been calibrated via a reference transducer. One calibration diagram is shown in figure 3 as an example. All output data of sensors have been collected by a 64 channel, 12 bit A/D board which is capable of data acquisition rate of 500 KHz. Raw data is filtered by a low-pass Bessel filter, using a cut-off frequency of 100 Hz.

Error calculation and uncertainty analysis

Bios error and precision of method are the most important reasons of error in the experimental studies. Uncertainty analysis is done in the boundary layer problems using the following equation[1].

$$\frac{B_u}{u} = \sqrt{(\frac{B_{\Delta v}}{2\Delta v})^2 + (\frac{B_\rho}{2\rho})^2 + (\frac{B_s}{2s})^2}$$

Where

$B_{\Delta v}$: maximum error due to electronic devices,

B_ρ: maximum error due to density changes during test,

B_S: maximum error of calibration slope,

Δv: voltage change,

ρ: density and

S: calibration slope.

Calculated from above formula, the maximum error is about 0.1%.

RESULT DISCUSSION

The results are discussed in various sections under the effect of different parameters. The experiments were conducted for angles of attack of -2, 0, 2 degree, and swept angles of 23, 33, 40 degrees. Moreover, the measurements were done in 3 different rake positions on each wing. At first, the points were located parallel to the quarter chord line of the model. Then the probes were moved to the root chord line, and finally they were moved perpendicular to the root chord. Figure 4 shows all wings and the positions of the measured points on the wing. At a constant tunnel velocity the boundary layer velocity is a function of the edge velocity and is independent of the free stream velocity. Note all experiments were performed at a free stream velocity of 50 m/s.

Velocity profile

The cross flow angle was not known exactly and unfortunately the rake that was present at the time of conducting the experiment could not measure this component. The rake could only measure the resultant velocities i.e. lateral (cross flow) and longitudinal (axial) components of velocity simultaneously.

It is evident that the flow behavior along the streamline is similar to that of the two dimensional boundary layers; the increase in the initial velocity was not expected. Therefore, the sudden increase in the measured velocity near the surface could be related to the increase in the cross flow component of the resultant velocity which is measured by the rake. As a result of this increase in the cross flow component, the resultant velocity has been increased.

Angle of attack

Figure 5 shows the effects of varying angle of attack for the 23 degree swept wing at a location close to the root. The highest maximum velocity is reached for angle of attack of -2°. So, the cross flow has maximum of its strength at -2° angle of attack. As the angle of attack is increased the cross flow strength decreases. And the lowest cross velocity appears at an angle of attack of -2°.

Moreover, the starting velocity of the profiles, measured at the height of 0.2mm from the surface shows the emergence of cross flow as well. In the vicinity of the surface there is a lower velocity, because the viscosity is highly dominant. At a slightly higher distance from the wing surface the cross flow immediately increases and causes a large increase in the total velocity, which is measured by rake. As the probes move further from the wing surface, the cross flow reduces again, and in the vicinity of boundary layer edge, its component becomes almost zero.

Swept angle

The effect of swept angle on the velocity profile at an angle of attack of -2° is shown in figure 6. The measured positions are for location of x/c=0.82-0.85 and 2y/b=0.2. The velocity profile shows that as the swept angle increases, the maximum velocity which represents the cross flow strength, increases. Increasing swept angle, increases the normal component of oncoming flow velocity, which is seen in figure 6. Note that as the wing swept angle increases, the differences between the pressure gradient term and the velocity vector increases too. Thus, the stream line should be curved more to balance the forces. This will result in stronger cross flow.

Tracing on the quarter chord line

Having a series of static pressure holes on the quarter chord line, this section seems to be an appropriate location to measure the velocity profile. Figure 7 shows the velocity profiles along the quarter chord line of this wing. For the 33° swept wing all the measured points have the same velocity profile along the quarter line. Also, the angle of flow is in the

direction of C/4 line. Moreover, the starting slope of the profile is almost constant. This slope represents the turbulence condition over the wing surface. The starting slope of the laminar profile is greater than that of the turbulence one. As this slope is constant along quarter chord line of the wing, it seems that the turbulence condition in this section is constant. Thus, it can be guessed that the transition line is parallel to quarter chord line.

Tracing parallel to the chord line

In this section, all measured points have the same 2y/b and the points trace from the leading edge to the trailing edge. Figure 8 shows the velocity profile for the 33° swept wing for all points parallel to the chord line. According to the figure, as the measured points get closer to the trailing edge, the maximum velocity in the profile decreases. It means that as x/c increases, the cross flow velocity decreases. The most powerful cross flow appears in the leading edge regions, and due to the viscose effects, the cross flow strength decreases in the trailing edge regions. Also, at the vicinity of the wall (first probe) the velocity has been decreased due to reduction of the cross flow component. All the profiles will reach the edge velocity at a height of 4 mm roughly.

The other significant point in this investigation is the starting slope of the profile. As shown in figure 8, this slope is greater in the leading edge than that in the trailing edge. As mentioned before, this slope could represent the turbulence condition of the flow over the wing surface. It is observed that as x/c increases sufficiently, the flow over the wing becomes turbulent.

Tracing perpendicular to the chord line

The measured points, have fixed x/c_{root}. Velocity profiles for the 33° wing, for points perpendicular to the chord at a position of x/c=0.82 are shown in figure 9. The reason for such a phenomenon is due to the fact that the measurement is in the vicinity of the wing leading edge. For swept wings, as the measuring point is moved from the tip toward the root along a line perpendicular to the chord, the present case, one gets closer to the wing leading edge too, the movement can be considered almost two dimensional. As the measurement point approaches the leading edge, the maximum velocity in the boundary layer profile near the surface increases.

Power spectra analysis

The data for four closest probes to the surface and that of the probe number 20 which are located out of boundary layer have been selected for spectrum analysis. In this condition, it is possible to compare the power spectra information for the inside and the outside of the boundary layer. To analyze the raw data “Discrete Fourier Theory” has been used.

Comparison of probe data across the boundary layer

Figure 10 shows the power spectra of five selected probes in this experiment, for 23° swept wing at -2° angle of attack. The measurements were performed at a fixed point. The amplitude of graphs exactly matches to the velocity of the points. As the velocity in profiles increases, the amplitude of power spectrum becomes higher. For example probe number 3 has the maximum velocity in profiles. Thus, in the power spectrum graph, it has the highest amplitude. The perturbation level in probe number 2 is less than that of other probes. The probe number 2 is very close to the surface and it seems that the viscosity has damped the perturbations at that region. There are 3 frequencies, having more amplitude than other, 0.6, 4 and 6 Hz, figure 10. The 0.6 and 6 Hz. Perturbation frequencies exist both inside and outside the boundary layer. Respectively, it shows that they are dependent to other sources than the boundary layer aerodynamic properties. On the other hand, these two frequencies are seen in all figures. So, they do not occur randomly. In fact these two frequencies were always along with the experiments, having external sources. Fan blade and very small vibration of rake might be two sources for these frequencies. They may occur due to the perturbation of the free stream or turbulence mode of wind tunnel.

The 4 Hz frequency is not seen in the probe number, or at least is not dominant. But it exists in other graphs with different amplitudes. In the next sections the source of 4 Hz frequency will be investigated.

Effect of the angle of attack

The effects of changing the angle of attack on the 3rd probe for the 23° swept wing at a point close to the root of the wing are shown in figure 11. Probe number 3 has the maximum velocity, thus, it has sufficient cross flow properties. The amplitude of perturbation is maximized at an angle of attack -2°, because the velocity at -2° angle of attack is more than that for other angles of attack. A frequency peak of 4 Hz is seen which is stronger at -2° angle of attack than other angles of attack. It could be guessed that, this frequency, 4 Hz, represents the cross flow instability.

Effect of the swept angle

As mentioned in the previous section, increasing the swept angle, causes an increase in the cross flow velocity. Figure 2 shows the power spectra of wing at -2° angle of attack for a point located at x/c=0.82-0.85 and 2y/b=0.2 which is close to the root. The results showed that a frequency of 4 Hz represents the cross flow instability.

Displacement parallel to the chord line

Figure 13 shows the power spectrum for 23° swept wing at 2y/b=0.2 and at the angle of attack of -2°. The points are located parallel to chord line. The points which are closer to the leading edge have higher amplitude. As x/c increases, the amplitude and peak of the 4 Hz frequency decreases. This can be due to the turbulence flow.

Displacement perpendicular to the chord

Getting closer to the tip, the amplitude of perturbation increases as is shown in figure 14. As mentioned before by increasing the velocity, the perturbation amplitude will increase. Figure 14 is for 23° swept wing at -2° angle of attack and the measurements were performed at x/c=0.83.

CONCLUSION

The experimental tests over a few isolated swept wings were undertaken to investigate the boundary layer velocity profile. The results showed that as the angle of attack increases, the cross flow velocity decreases and so the cross velocity is stronger at lower angles of attack. Also, increasing the swept angle causes an increase in the cross velocity. It seems that the cross flow is very stronger at the leading edge than at the trailing edge. Because as x/c increases the cross flow velocity decreases. The slope of the profile in the vicinity of the surface decreases, as x/c increases. It means that the flow is near the turbulent condition. The velocity of the cross flow, however, is nearly constant. The power spectra analyses showed higher amplitude at higher velocities and a frequency of 4 Hz might be guessed as the cross flow instability frequency.

REFERENCES

[1] Barlow J.B., and Rae W.H., Pope A., Low Speed Wind Tunnel Testing, Third Edition, John Wiley & Sons, 1999.

[2] M.R. Soltani, K. Ghorbanian, M. Masdari, M. Seiedjafari, “Investigation of the pressure distribution and transition point over a swept wing”, Sharif university of technology, 2010.

[3] Stuart, J. T., "The Basic Theory of the Stability of Three- Dimensional Boundary Layers", Rep. No. F.M. 1899, British Natl. Phys. Lab. (Rep. No. 15, 904, A.R.C.), May, 1953.

[4] Hillissy B. James, Philips S. Pamela, Wind Tunnel Investigation of Aerodynamic Characteristics and Wing Pressure Distribution of an Airplane with Variable Swept Wings Modified for Laminar Flow, Langley research center Hampton Virginia, 1989, NASA Technical memorandom 4124.

[5] J. Ray Dagenhart, William S. Saric, Crossflow Stability and Transition Experiments in Swept-Wing Flow, NASA/TP-1999-209344, July 1999.

[6] Tuncer Cebeci, Jean Cousteix, Modeling and Computation of Boundary-Layer Flows, Springer, 2005

[7] Joseph A. schetz, Boundary layer analysis, prentice hall Inc., 1993.

[8] White. E. B., Saric, W. S., Gladden, R. D., Gabet, P. M., “Stages of Swept-Wing Transition”, AIAA, 2001.

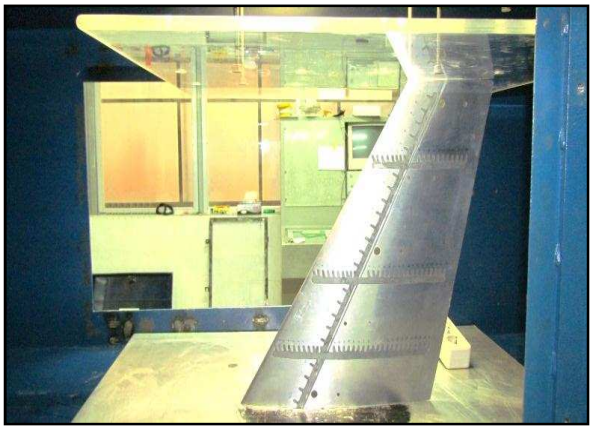

Figure 1- Model in the wind tunnel

Figure 2- Rake`s tilting mechanism

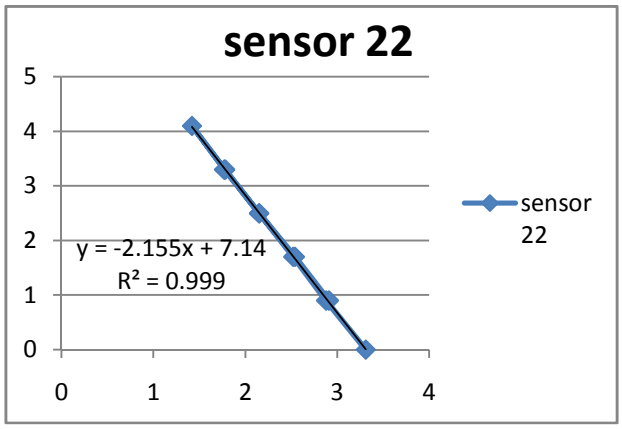

Figure 3- Calibration diagram for sensor 22

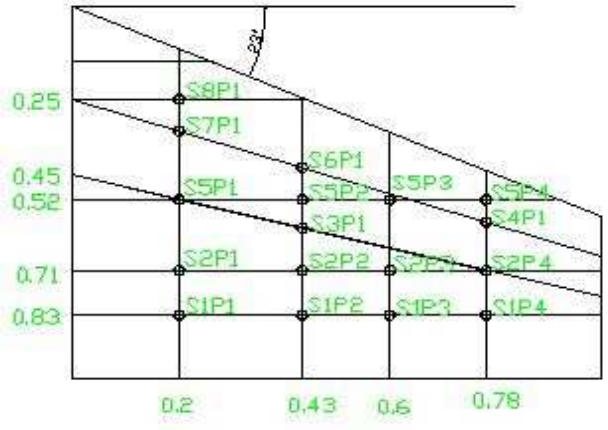

a) Swept angle 23 degree

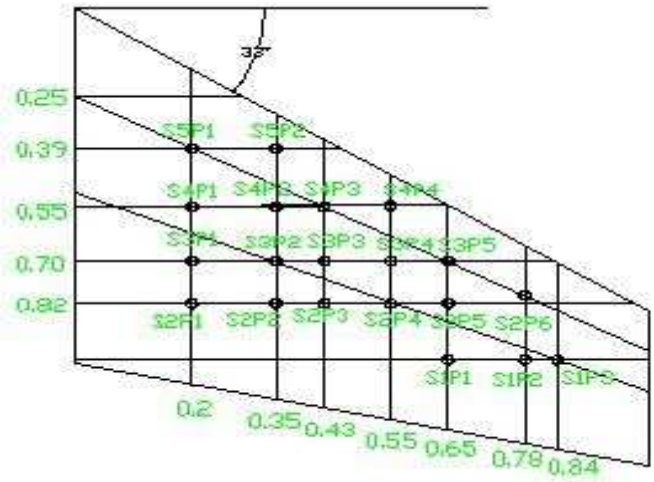

b) Swept angle 33 degree

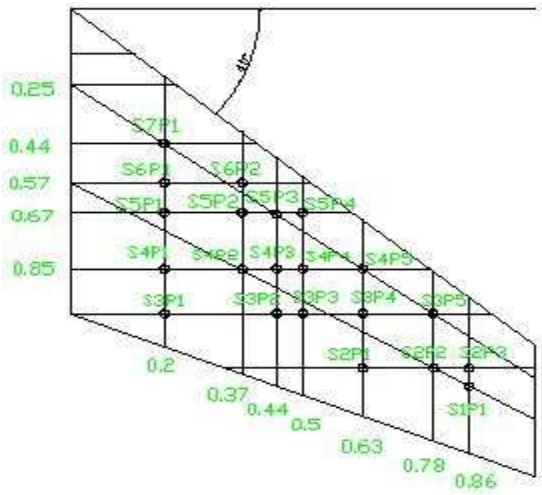

c) Swept angle 40 degree

Figure 4- Drawings of wings and the measuring positions

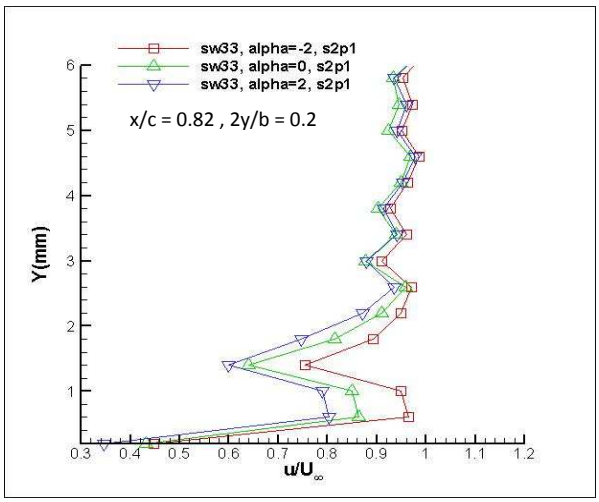

Figure 5- Velocity profile for the 33° swept wing at various angles of attack

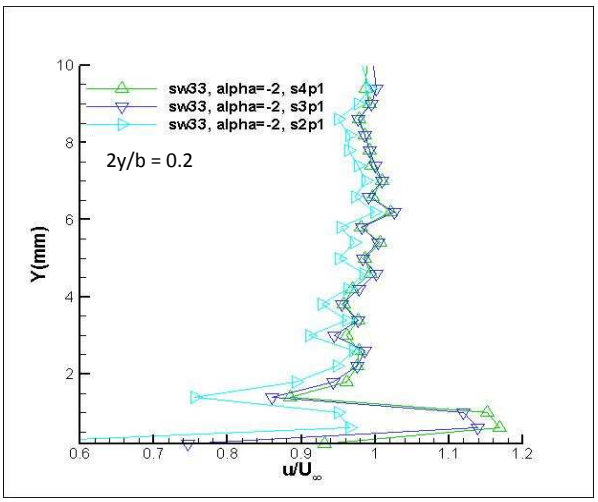

Figure 8- Velocity profile for the 33° swept wing at α=-2° along 2y/b=0.2

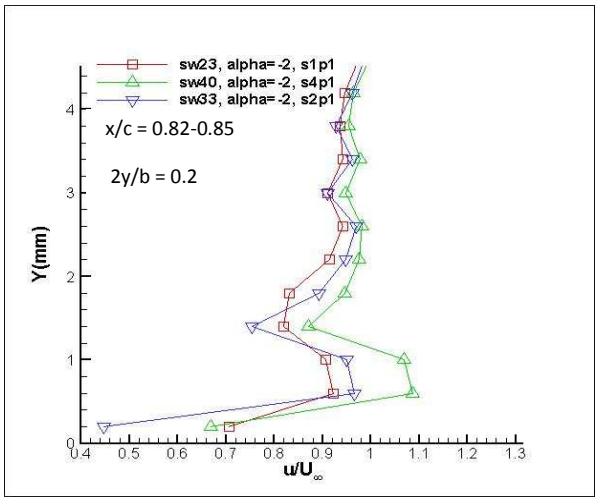

Figure 6- Effect of sweep on velocity profile, α=-2°

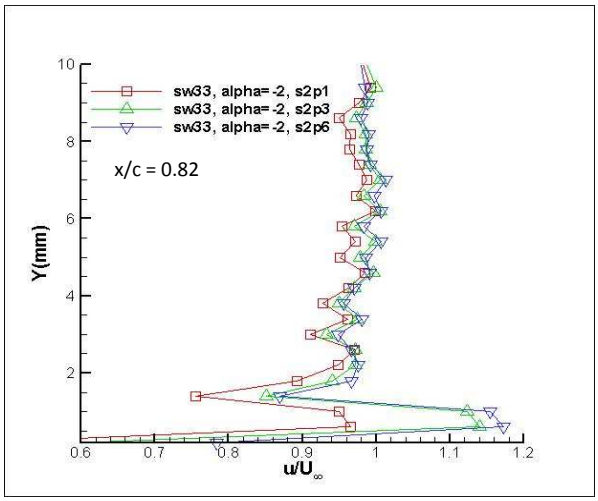

Figure 9- Velocity profile for the 33° swept wing at α=-2° along x/c=0.82

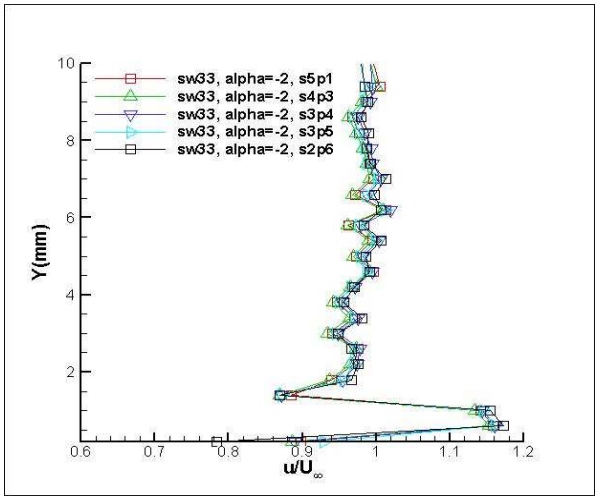

Figure 7- Velocity profile for the 33° swept wing along its quarter chord line

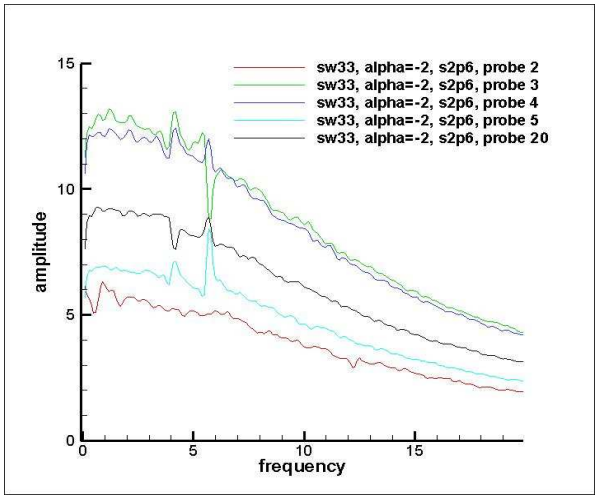

Figure 10- Power spectrum for the 33° swept wing for different probes

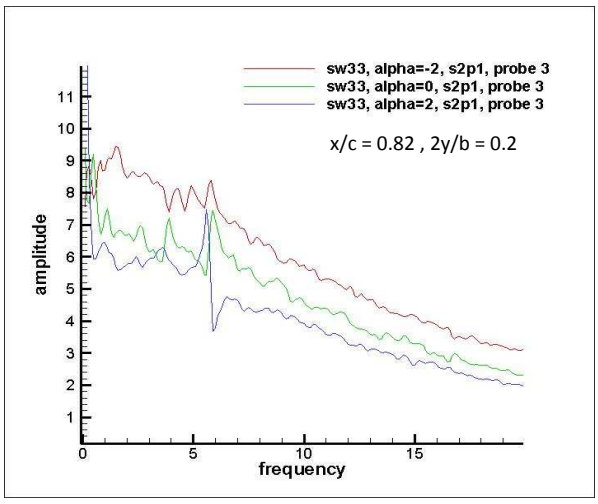

Figure 11- Power spectrum of the 33° swept for the probe no. 3, x/c=0.82, 2y/b=0.2

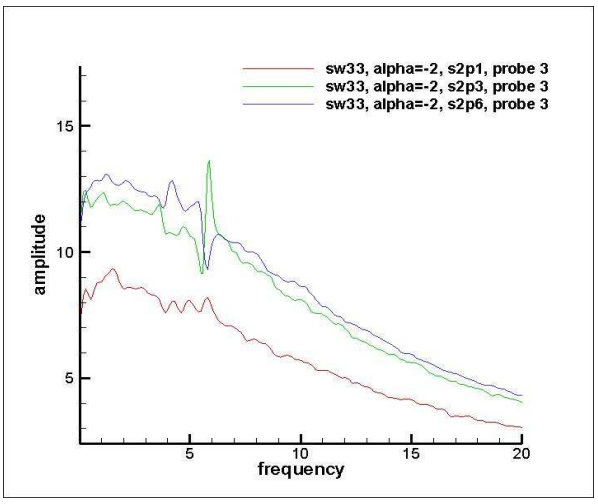

Figure 14- Power spectrum of 33° swept wing at α=-2°, along x/c=0.82

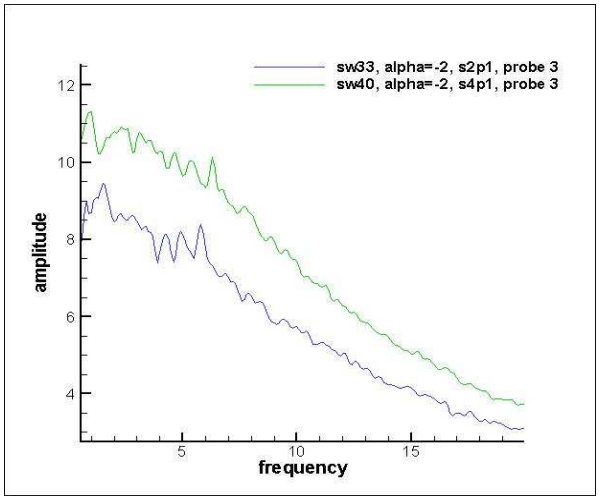

Figure 12- Power spectrum of 33° and 40° swept wings at α=-2°, probe no. 3

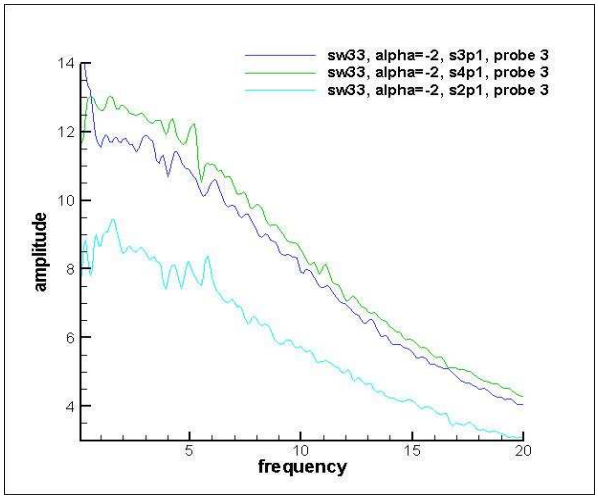

Figure 13- Power spectrum of 33° swept wing at α=-2°, along 2y/b=0.2